Earth and Planetary Science Letters 285 (2009) 283–296

Contents lists available at ScienceDirect

Earth and Planetary Science Letters

journal homepage: www.elsevier.com/locate/epsl

The tectonics of Mercury: The view after MESSENGER's first flyby

Thomas R. Watters [a,*], Sean C. Solomon [b], Mark S. Robinson [c], James W. Head [d], Sarah L. André [e], Steven A. Hauck II [f], Scott L. Murchie [g]

[a] Center for Earth and Planetary Studies, National Air and Space Museum, Smithsonian Institution, Washington, DC 20560, USA
[b] Department of Terrestrial Magnetism, Carnegie Institution of Washington, Washington, DC 20015, USA
[c] School of Earth and Space Exploration, Arizona State University, Tempe, AZ 85251, USA
[d] Department of Geological Sciences, Brown University, Providence, RI 02912, USA
[e] Center for Earth and Planetary Studies, National Air and Space Museum, Smithsonian Institution, Washington, DC 20560, USA
[f] Department of Geological Sciences, Case Western Reserve University, Cleveland, OH 44106, USA
[g] Space Department, Johns Hopkins University Applied Physics Laboratory, Laurel, MD 20723, USA

ARTICLE INFO

Article history:
Received 3 September 2008
Received in revised form 13 January 2009
Accepted 13 January 2009
Available online 28 February 2009

Edited by: T. Spohn

Keywords:
Mercury
MESSENGER
tectonics
lobate scarp
wrinkle ridge
graben

ABSTRACT

During its first flyby of Mercury, MESSENGER imaged many tectonic landforms, most of which are contractional in nature and include lobate scarps, high-relief ridges, and wrinkle ridges. Wrinkle ridges are found on the smooth plains that partially fill the interior and surround the exterior of the Caloris basin and also on smooth plains that fill the interiors of smaller impact basins and larger craters. MESSENGER revealed a radial graben complex, Pantheon Fossae, nearly co-centered with the Caloris basin. Pantheon Fossae and a network of mostly basin-concentric graben in the outer portions of the Caloris basin interior form a pattern of extension not seen elsewhere on Mercury. The first clear example of extensional faults outside of the Caloris basin has been documented on smooth plains inside the peak ring of the relatively young Raditladi basin. A map of the distribution of tectonic landforms imaged by MESSENGER and Mariner 10 shows that lobate scarps are the most widespread type of feature. Estimates of the horizontal shortening associated with lobate scarps that crosscut and overthrust small impact craters imaged by MESSENGER range from ~1 to 3 km. Previously unrecognized lobate scarps detected in areas imaged by Mariner 10 indicate that earlier estimates of contractional strain are low. A new estimate of the average areal contractional strain (~0.06%) accommodated by scarps is at least one third greater than comparable previous estimates and corresponds to a decrease in Mercury's radius of at least 0.8 km since the end of heavy impact bombardment of the inner solar system. These figures are lower bounds because of the likelihood that not all lobate scarps have been identified even in areas imaged to date. Crosscutting and embayment relations revealed by MESSENGER suggest that lobate scarps formed before the end of smooth plains emplacement and continued to be active after the emplacement of the youngest smooth plains deposits. Relatively recent activity on lobate scarps may be the expression of slow but continuous radial contraction that accompanied cooling of Mercury's interior and the growth of the planet's solid inner core.

Published by Elsevier B.V.

1. Introduction

The history of crustal deformation on Mercury has important implications for interior thermal history models, the cooling of the planet's mantle, and the growth of the solid inner core. Until the first flyby of Mercury by the MErcury Surface, Space ENvironment, GEochemistry, and Ranging (MESSENGER) spacecraft in January 2008 (Solomon et al., 2008), our knowledge of the tectonics of Mercury was derived from images obtained by Mariner 10 more than 30 years ago. In three flybys in 1974–1975, Mariner 10 imaged about 45% of the planet's surface, and for only about half of the imaged area were incidence angles favorable to the identification of low-relief morphological features. During its first flyby of Mercury, MESSENGER viewed about 21% of the surface not seen by Mariner 10, and on both approach and departure MESSENGER imaged portions of the surface viewed by Mariner 10 but under different illumination conditions. In this paper, we make use of images obtained during MESSENGER's first Mercury flyby to extend our understanding of the global tectonics of Mercury derived from Mariner 10 observations and to explore the implications of the new observations for the thermal evolution of the innermost planet.

We begin with a brief summary of the state of knowledge of the tectonic history of Mercury derived from Mariner 10 observations, and we follow with a description of the tectonic landforms newly imaged by MESSENGER. On the basis of a map of these tectonic features, in combination with those previously recognized from Mariner 10 images, we assess their spatial distribution and their relation to other geological features and units. We describe examples where embayment and superposition relations provide improved constraints on the timing of lobate scarp formation and activity. Finally, from estimates for the

* Corresponding author.
E-mail address: watterst@si.edu (T.R. Watters).

0012-821X/$ – see front matter. Published by Elsevier B.V.
doi:10.1016/j.epsl.2009.01.025

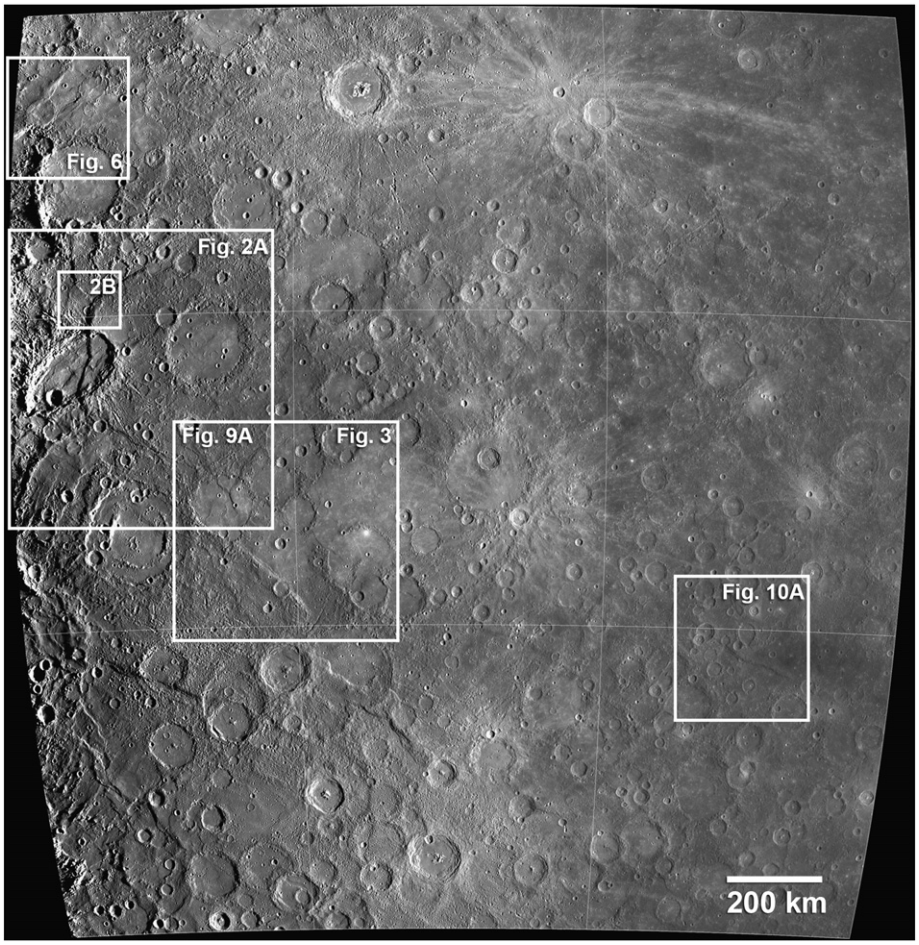

Fig. 1. MESSENGER NAC mosaic of part of Mercury's surface not seen by Mariner 10, depicting the locations of images shown in several other figures in this paper. The mosaic covers the area from 30°S to 15°N and 96°E to 141°E and was constructed with images acquired on departure from closest approach. The locations of Figs. 2A, B, 3, 6, 9A, and 10 are indicated. A 15°×15° grid of latitude and longitude is shown in white. The resolution of the mosaic is ~530 m/pixel.

horizontal shortening and contractional strain expressed by known lobate scarps, we provide an updated constraint on the amount of global contraction accumulated since the end of heavy bombardment and its implication for interior thermal history models.

2. Background

Evidence of broadly distributed crustal deformation on Mercury was revealed in Mariner 10 images by three types of tectonic landforms: lobate scarps, high-relief ridges, and wrinkle ridges. Lobate scarps are linear or arcuate landforms generally asymmetric in cross-section with a steeply sloping scarp face and a gently sloping back limb (Strom et al., 1975; Cordell and Strom, 1977; Dzurisin, 1978; Melosh and McKinnon, 1988; Watters et al., 1998). Offsets of the walls and floors of transected impact craters suggest that the scarps are the expression of surface-breaking thrust faults (Strom et al., 1975; Cordell and Strom, 1977; Melosh and McKinnon, 1988; Watters et al., 1998, 2001). High-relief ridges are more symmetric in cross-section and, like lobate scarps, deform the walls and floors of the impact craters they transect, suggesting that they are also formed by reverse faults (Watters et al., 2001, 2004; Watters and Nimmo, in press). Wrinkle ridges are complex morphologic landforms often consisting of a broad, low-relief arch with a narrow superimposed ridge interpreted to be formed by a combination of folding and thrust faulting (Golombek et al., 1991; Watters, 1988; Schultz, 2000). The most prominent and widely distributed of these tectonic features in the Mariner 10 images are the lobate scarps. The only clear evidence for crustal extension in the areas of Mercury imaged by Mariner 10 was found in the interior plains of the Caloris basin, where troughs arrayed around the outer reaches of the basin interior were interpreted to be graben (Strom et al., 1975; Dzurisin, 1978; Melosh and McKinnon, 1988; Watters et al., 2005; Watters and Nimmo, in press).

The timing of deformation can be constrained by the stratigraphy and crater retention ages of the geological units that have been faulted (Spudis and Guest, 1988). Geological terrains on Mercury have been grouped into five time-stratigraphic systems, for which approximate ages have been estimated by extrapolation from the lunar cratering flux history; those systems are the pre-Tolstojan (older than approximately 4 Ga), followed by Tolstojan (~4.0–3.9 Ga), Calorian (~3.9–3.5 Ga), Mansurian (~3.5–3.0 Ga), and Kuiperian (~1.0 Ga) (Spudis and Guest, 1988). In the areas viewed by Mariner 10, lobate scarps deform pre-Tolstojan plains material – intercrater plains, emplaced before the end of the heavy impact bombardment of the inner solar system – as well as youngest Calorian-aged smooth plains units. Thus, although the onset of lobate scarp formation is not well constrained, scarp activity continued until after the emplacement of the youngest smooth plains (Strom et al., 1975; Melosh and McKinnon, 1988). Additional arguments that many of the lobate scarps seen by Mariner 10 were active in the Calorian include the following: (1) there is no evidence from Mariner 10 images of embayment of scarps by ancient intercrater plains (Melosh and McKinnon, 1988) or by Tolstojan and Calorian smooth plains materials (Watters et al., 2004), (2) lobate scarps often crosscut and offset the floors and rim walls of large impact craters (Fig. 1), (3) no large craters are

superimposed on lobate scarps, and (4) no obvious degradation or partial burial of lobate scarps by Caloris ejecta is seen (Watters et al., 2004).

Models for the lithospheric stresses that produced the observed distribution of tectonic features viewed by Mariner 10 have involved some combination of global contraction accompanying interior cooling, tidal despinning, and stresses related to the formation and modification of the Caloris basin (Strom et al., 1975; Solomon, 1976, 1977, 1978, 1979; Cordell and Strom, 1977; Melosh, 1977; Melosh and Dzurisin, 1978; Pechmann and Melosh, 1979; Melosh and McKinnon, 1988; Thomas et al., 1988; Schubert et al., 1988; Phillips and Solomon, 1997; Hauck et al., 2004; Dombard and Hauck, 2008; Matsuyama and Nimmo, 2009). Patterns of lithospheric stress for each of these models predict specific spatial and temporal distributions of contractional faults and their associated lobate scarps. Contraction of the planet from interior cooling, absent other influences, would result in global, horizontally isotropic compressive stress and a more or less uniformly distributed population of lobate scarps with no preferred orientation or thrust direction (e.g., Watters et al., 2004). The onset of lithospheric contraction is predicted to occur before the end of heavy bombardment for most thermal history models (Solomon, 1976, 1977, 1978, 1979; Schubert et al., 1988; Hauck et al., 2004; Dombard and Hauck, 2008).

The predicted stresses from tidally induced despinning and the relaxation of an early equatorial bulge (Melosh, 1977; Melosh and Dzurisin, 1978; Melosh and McKinnon, 1988) would be expected to result in north-south-oriented thrust faults near the equator and east-west-oriented normal faults in polar regions (Melosh, 1977). Extension in Mercury's polar regions predicted by tidal despinning has not been observed (Solomon, 1978; Melosh and McKinnon, 1988; Schubert et al., 1988; Watters et al., 2004). Stresses from tidal despinning and contraction may have been coupled if the two processes overlapped in time (Pechmann and Melosh, 1979; Melosh and McKinnon, 1988; Dombard and Hauck, 2008; Matsuyama and Nimmo, 2009; Watters and Nimmo, in press). Dombard and Hauck (2008) drew attention to the possibility that early tidal despinning and global contraction led to a population of north-south-oriented thrust faults that, although rendered unrecognizable by heavy bombardment, may have been reactivated by subsequent global contraction as the planet continued to cool. Matsuyama and Nimmo (2009) emphasized the possible importance of polar wander resulting from the formation and infilling of the Caloris basin and found that the orientations of thrust faults predicted for a combination of such polar wander with contraction and despinning are, under some assumptions, in broad agreement with those observed by Mariner 10 as well as with limited information on the planet's long-wavelength gravity field. Thomas et al. (1988) suggested that lithospheric stresses from thermal contraction may have interacted with stresses associated with the formation of the Caloris basin, resulting in Caloris-radial thrust faults, but few lobate scarps in areas imaged by Mariner 10 are radial to the Caloris basin.

Convection in Mercury's mantle may have imparted additional stresses to the lithosphere during the time of lobate scarp formation (Watters et al., 2004; King, 2008; Watters and Nimmo, in press). In three-dimensional models of convection in Mercury's mantle, the pattern of mantle downwelling can lead to predominantly east-west compression at low latitudes and generally north-south compression in the polar regions (King, 2008). This pattern of stresses is broadly consistent with the orientations of mapped lobate scarps in areas imaged by Mariner 10 (Watters et al., 2004). Stress from global contraction, however, must be sufficiently large to prevent extension in regions of mantle upwelling, and the magnitude of the predicted stresses would result in large dynamic topography that is not observed (Watters and Nimmo, in press).

3. MESSENGER imaging observations

The Mercury Dual Imaging System (MDIS) (Hawkins et al., 2007) obtained images on approach to and departure from Mercury during the MESSENGER flyby of 14 January 2008. The highest-resolution images were obtained with the MDIS narrow-angle camera (NAC). The NAC approach images have resolutions down to ~485 m/pixel, and the NAC departure images have resolutions down to ~120 m/pixel, obtained just after closest approach. Mosaics of the NAC approach and departure sequences have been used to identify and map the location of tectonic features. The optimum lighting geometry for the detection of tectonic landforms is at large solar incidence angles, approximately 60° to 85° measured from nadir, and occurs within about 35° longitude of the terminator on the approach and departure hemispheres. To extend areal coverage, however, tectonic features have been identified in MESSENGER images at incidence angles as small as 40°.

4. Tectonic landforms

4.1. Lobate scarps

The most prominent lobate scarp viewed during MESSENGER's first flyby is Beagle Rupes (Figs. 1, 2), over 600 km long and one of the most arcuate of the lobate scarps found on Mercury to date (Solomon et al., 2008). The north–south-trending segment of Beagle Rupes

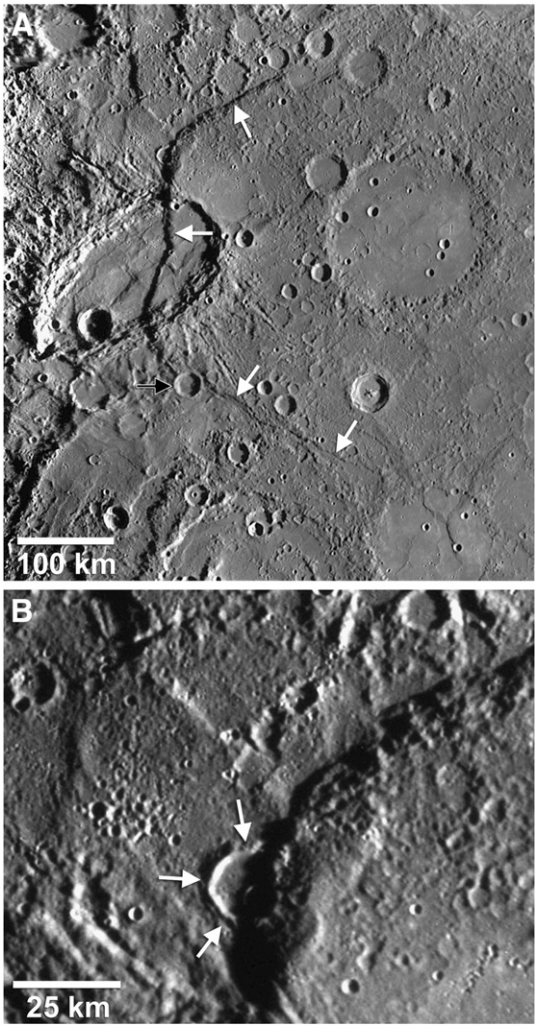

Fig. 2. Beagle Rupes, an arcuate lobate scarp imaged by MESSENGER. (A) The scarp (white arrows) is over 600 km long and offsets the floor and walls of the eccentric Sveinsdóttir impact crater. The floor of Sveinsdóttir was flooded by smooth plains and subsequently deformed by wrinkle ridges prior to being crosscut by the thrust fault. A ~27-km-diameter crater sits undeformed on the northwest-southeast segment of the scarp (black arrow). The resolution of the mosaic is ~530 m/pixel. (B) The northern segment of Beagle Rupes crosscuts a ~17-km-diameter impact crater (white arrows) formed in intercrater plains. The resolution of the image is 210 m/pixel. The locations of (A) and (B) are shown in Fig. 1.

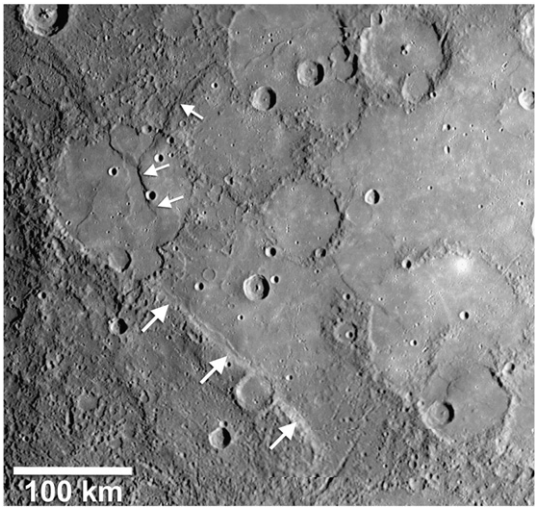

Fig. 3. Several lobate scarps imaged by MESSENGER. Smooth plains material appears to have ponded against the structural relief of a preexisting linear lobate scarp formed in older intercrater plains (lower set of thick white arrows). A second lobate scarp (upper set of thin white arrows) cuts across both intercrater plains and smooth plains that filled the floor of a ~120-km-diameter impact crater. The location of this NAC mosaic is shown in Fig. 1. The resolution of the mosaic is ~530 m/pixel.

crosscuts the elliptically shaped Sveinsdóttir crater. With a long axis of ~220 km and a short axis of ~120 km, the crater is one of the largest impact features on Mercury crosscut by a lobate scarp. An important aspect of Sveinsdóttir is that its floor was flooded by smooth plains material that was subsequently deformed by wrinkle ridges, many with orientations that are subparallel to the crater's long axis (Fig. 2A). The last stage in the deformation of Sveinsdóttir appears to be when it was crosscut by Beagle Rupes, which offset the basin walls and the interior smooth plains. There are two other key superposition relations involving Beagle Rupes and impact craters. One occurs to the north of the rim of Sveinsdóttir, where a ~17-km-diameter impact crater has been deformed by the north–south-trending segment of Beagle Rupes (Fig. 2B), and the other is south of Sveinsdóttir, where a ~27-km-diameter crater is superposed on the northwest-southeast trending segment of Beagle Rupes (Fig. 2A).

Like other large lobate scarps on Mercury, Beagle Rupes has significant topographic relief. The maximum relief of the scarp just south of the deformed 17-km-diameter crater is over 1.5 km on the basis of shadow measurements (Fig. 2B). Such relief is comparable to that of Discovery Rupes (Watters et al., 1998), one of the largest lobate scarps imaged by Mariner 10. The maximum relief of the portion of Beagle Rupes within Sveinsdóttir crater, where the scarp offsets the interior smooth plains, is ~800 m, also from shadow measurements.

Other lobate scarps occur to the southeast of Beagle Rupes (Fig. 3). The largest of these is a linear scarp ~200 km long. This landform has the basic characteristics of a lobate scarp, a relatively steeply sloping scarp face and a gently sloping back limb. The northwest–southeast orientation of the scarp approximately parallels that of the southernmost segment of Beagle Rupes. A ~30-km-diameter impact crater is crosscut by the scarp, leaving a small portion of the northeasternmost floor and rim offset from the portion of the crater on the scarp's backslope. An important aspect of this lobate scarp is that the scarp face coincides with the contact between intercrater plains to the southwest and smooth plains to the northeast (Fig. 3). This contact indicates that smooth plains material ponded against the preexisting structural relief of the lobate scarp that formed in older intercrater plains (Solomon et al., 2008). Flanking the scarp, just outward of the scarp face, is a series of low-relief ridges in the smooth plains. The northernmost segment of the linear lobate scarp extends nearly to the rim of a degraded ~120-km-diameter impact crater that has also been flooded by smooth plains. These smooth plains are likely associated with the broader-scale volcanic emplacement (Head et al., 2008) of smooth plains in the region (Fig. 1). The smooth plains interior to the crater were then deformed by wrinkle ridges having orientations that are generally radial to the rim (Fig. 3).

A ~160-km-long lobate scarp extends from intercrater plains to the northeast of the degraded crater into the interior smooth plains. Shadow measurements indicate that this lobate scarp has ~450 m of relief where it deformed the smooth plains. The formation of the lobate scarp clearly postdates the emplacement of the smooth plains, and the crosscutting relations between the scarp and a wrinkle ridge (Fig. 3) suggest that the thrust fault scarp postdates the formation of the wrinkle ridges (Solomon et al., 2008). Like Beagle Rupes, this lobate scarp has important superposition relations with two small impact craters. A ~9-km-diameter crater is superposed on the southernmost segment of the lobate scarp, and a ~5-km-diameter crater located near the northern rim of the degraded crater is crosscut by the scarp (Fig. 3). The fresh, undegraded appearance of both these craters suggests that they are Calorian age or younger.

The discovery of lobate scarps was not limited to areas seen for the first time by MESSENGER. From the NAC approach images of areas near the Mariner 10 subsolar longitude (where incidence angles were small), previously unrecognized tectonic features have been identified. One such newly recognized scarp is shown in Fig. 4. This ~270-km-long, arcuate lobate scarp deforms intercrater plains and crosscuts a large impact crater. The northern segment of the scarp cuts the southern rim and extends through the floor of a ~75-km-diameter crater. A second lobate scarp, laterally offset from the longer arcuate scarp, cuts across the floor of a larger (~120-km diameter), more heavily degraded crater (Fig. 4).

4.2. High-relief ridges

Of the three types of contractional tectonic features that have been identified on Mercury, high-relief ridges are the least common. Usually found in intercrater plains, they are long, approximately symmetric ridges (Dzurisin, 1978; Melosh and McKinnon, 1988; Watters et al., 2001, 2004; Watters and Nimmo, in press). Although high-relief ridges have significant relief, they are relatively broad landforms, and thus some are not easily

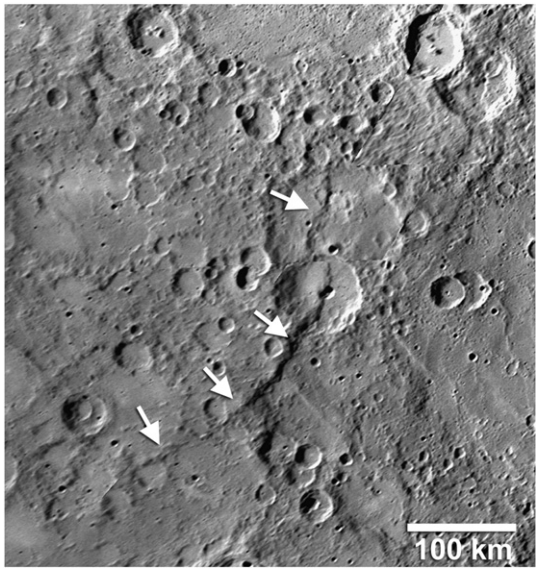

Fig. 4. Two newly recognized lobate scarps in an area imaged by Mariner 10. The bottom three arrows delineate a ~270-km-long arcuate lobate scarp that crosscuts a ~75-km-diameter impact crater (just north of the three arrows). This scarp was previously undetected because of the poor lighting geometry for the Mariner 10 images of the area. A second lobate scarp, laterally offset from the first, crosscuts a ~120-km-diameter impact crater (upper white arrow). This NAC mosaic is centered near 24°S, 254°E, and has a resolution of ~510 m/pixel.

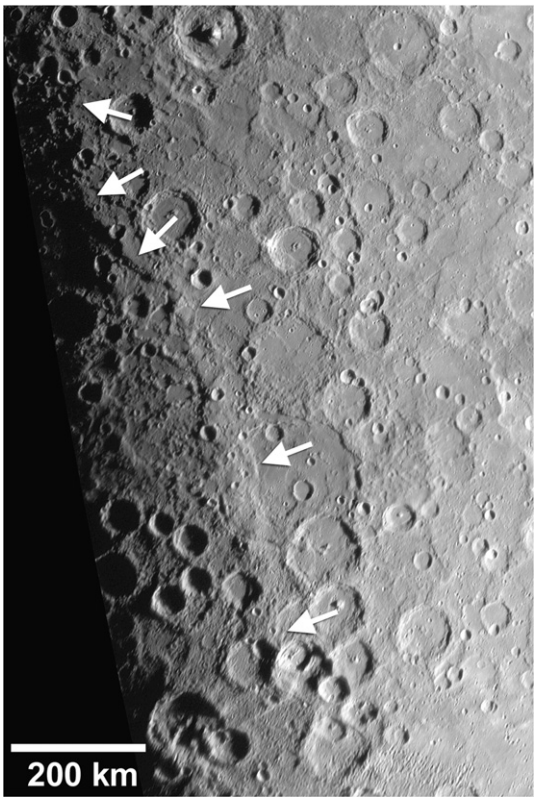

Fig. 5. A prominent high-relief ridge imaged by MESSENGER. The ridge is over 600 km in length (lower three white arrows). To the north, the ridge transitions into a lobate scarp that is ~400 km in length (upper three white arrows). The combined length of the two structures makes it the longest tectonic feature yet found on Mercury. This NAC mosaic is centered near 54°S, 107.5°E, and has a resolution of ~470 m/pixel.

detected in monoscopic images (Watters et al., 2001; Watters and Nimmo, in press). A remarkable high-relief ridge was imaged by MESSENGER on departure near the dawn terminator. The ridge is over 600 km long, has a maximum width of ~60 km, and is notably linear (Fig. 5). It cuts across a heavily degraded ~200-km-diameter impact feature and appears to have deformed both the interior fill and the western portion of the rim. To the north, the high-relief ridge transitions into an arcuate lobate scarp that is almost 400 km in length (Fig. 5). Transitions from high-relief ridge to lobate scarp have also been seen in Mariner 10 images (Watters et al., 2001; Watters and Nimmo, in press). The combined length of the high-relief ridge and lobate scarp is over 1000 km, making it the longest tectonic feature found on Mercury to date.

4.3. Wrinkle ridges

Smooth plains material on Mercury, whether within impact features or emplaced as broad plains, is commonly deformed by wrinkle ridges (Watters and Nimmo, in press). Wrinkle ridges on smooth plains within craters and basins are crosscut by lobate scarps in a number of areas imaged by MESSENGER (Figs. 2A, 3). They are also found in smooth plains that appear to have partially filled topographic lows in intercrater plains. Such a smooth plains unit viewed by MESSENGER has wrinkle ridges that display two common morphologic elements of the structure, a broad arch and a superposed ridge (Fig. 6). Two approximately parallel northeast–southwest-trending wrinkle ridges intersect a well-defined wrinkle-ridge ring ~60 km in diameter. A single wrinkle ridge, also with a northeast–southwest orientation, intersects the ridge ring on the

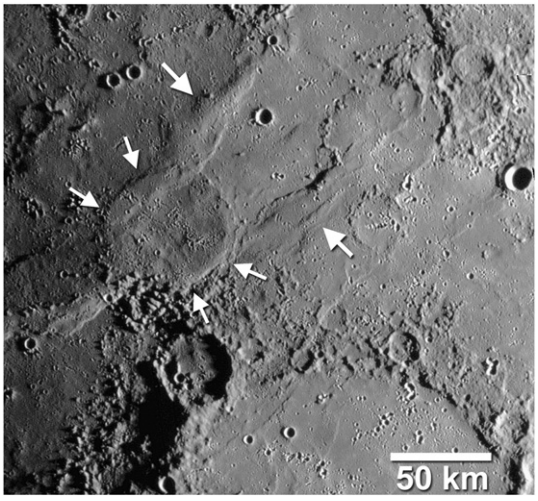

Fig. 6. Wrinkle ridges and a wrinkle-ridge ring in smooth plains material. Two subparallel wrinkle ridges trending approximately northeast-southwest show evidence of broad, low-relief arches with superposed ridges, landforms typical of planetary wrinkle ridges (upper large white arrows). The wrinkle-ridge ring (lower small white arrows) reflects the influence of a buried impact crater (Head et al., 2008). The resolution of this mosaic is ~530 m/pixel; its location is shown in Fig. 1.

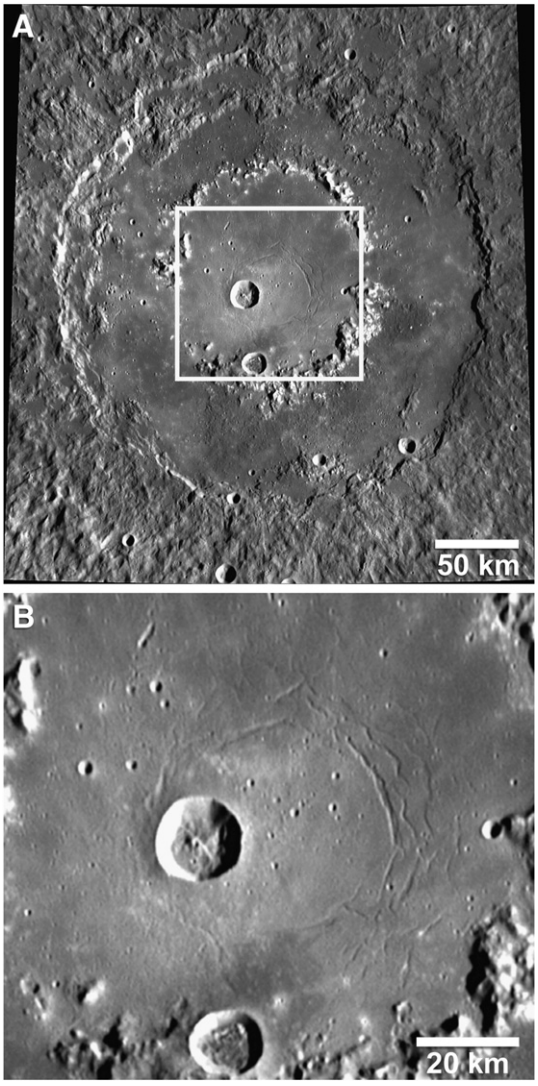

Fig. 7. Extensional troughs in the Raditladi basin. (A) The Raditladi basin is ~250 km in diameter and has a well-developed peak-ring structure ~120 km in diameter. The interior of Raditladi has been partially filled by smooth plains material. The mosaic is centered at 27°N, 119°E, and has a resolution of 210 m/pixel. (B) Concentric troughs in the floor material interior to the peak ring are interpreted to be graben. The location of (B) is shown in (A).

opposite side. Wrinkle-ridge rings are common structures in mare basalt units on the Moon and in ridged plains on Mars (Watters, 1988, 1993; Head et al., 2008). The rings likely overlie buried impact craters whose shallow rim crests acted as mechanical discontinuities that served to concentrate near-surface stresses.

4.4. Extensional troughs

Prior to the MESSENGER flyby, the only definitive evidence of extensional faulting on Mercury was in the eastern portion of the Caloris basin interior plains, where troughs concentric and radial to the basin center are interpreted to be graben indicative of uplift of the basin floor (Strom et al., 1975; Melosh and McKinnon, 1988; Watters et al., 2005). It was not known if the troughs seen in the outer reaches of the eastern basin floor in Mariner 10 images occurred elsewhere in the basin. MESSENGER has now provided the first complete view of the Caloris basin. One of the most remarkable results of the MESSENGER flyby was the discovery of a radial graben complex, Pantheon Fossae, interior to and converging to a locus near the center of the Caloris basin (Murchie et al., 2008). Graben from this radial complex are now known to extend to the assemblage of basin-concentric and basin-radial graben that continue around the entire outer reaches of the Caloris basin interior (Murchie et al., 2008; Watters et al., 2009-this issue). Hypotheses for the origin of the extension of the Caloris basin floor, and of the Pantheon Fossae in particular, are treated in companion papers (Freed et al., 2009-this issue; Head et al., 2009-this issue; Watters et al., 2009-this issue).

Outside of the Caloris basin, the only other extensional deformation seen in MESSENGER images occurs within the comparatively young ~250-km-diameter Raditladi basin (Strom et al., 2008). The floor of Raditladi contains smooth plains material, presumably volcanic in origin, which partially fills the basin and embays its prominent peak-ring structure (Fig. 7A). The smooth plains interior to the peak ring have a set of troughs (Fig. 7B) that clearly resemble those in the Caloris basin and are interpreted to be graben. The graben are approximately concentric to the peak ring and are confined to a small portion of the interior basin floor. As in the case of Caloris, these graben are likely the result of post-impact uplift of the basin floor (Murchie et al., 2008; Solomon et al., 2008).

5. Distribution of tectonic features

To evaluate the spatial distribution of tectonic features imaged by MESSENGER, their locations have been digitized directly from map-projected NAC image mosaics. Identified tectonic landforms are divided into segments on the basis of orientation, with segment lengths generally greater than 5 km. Segments of tectonic features were digitized and coded according to the structure type (e.g., lobate scarp, high-relief ridge, wrinkle ridge, extensional trough). This compilation includes tectonic features not previously recognized in images obtained by Mariner 10. Combining digitized tectonic features imaged by MESSENGER with those previously imaged by Mariner 10 (Watters et al., 2004; Watters and Nimmo, in press) provides the most comprehensive view of the distribution of tectonic features on Mercury to date (Fig. 8). The tectonic feature map covers about 66% of the surface of Mercury.

Several important observations can be made about the number and distribution of tectonic features. First, lobate scarps are the dominant tectonic landform on Mercury (Fig. 8A). Second, the distribution of recognized lobate scarps and other tectonic landforms is not uniform. There are four conspicuous concentrations of tectonic features that occur in longitudinal bands, separated by bands where there are distinctly fewer tectonic features. The apparent gaps are strongly correlated with areas of the surface imaged under poor lighting conditions (small solar incidence angles). This correlation is clearly evident when the tectonic features are plotted on a combined MESSENGER and Mariner 10 image mosaic (Fig. 8B). The limitations of poor lighting geometry on the identification and mapping of tectonic features is well demonstrated in the area surrounding the Mariner 10 subsolar point (near 0°N, 250°E). A scarcity of tectonic features identified in this region from Mariner 10 images was previously noted (Watters et al., 2004, Fig. 2). Most of the tectonic features shown in the longitudinal band between ~240°E and 270°E (the area around the Mariner 10 subsolar longitude) have been identified from the MESSENGER approach NAC image sequence (Fig. 8A, B).

Another important aspect of the distribution of tectonic features is the difference between the northern and southern hemispheres. The number of tectonic landforms in the southern hemisphere is larger than in the northern hemisphere (Fig. 8A). Also, a majority of the largest lobate scarps and high-relief ridges known on Mercury is found in the southern hemisphere. This asymmetry was noted in an earlier analysis of the distribution of tectonic features as seen by Mariner 10 (Watters et al., 2004). Differences in the number and scale of tectonic features as functions of latitude can be consequences of variations in lighting conditions, but the viewing conditions for the MESSENGER flybys were not substantially different for the northern and southern hemispheres.

The Caloris basin is a conspicuous feature on the tectonic map because of the large concentration of wrinkle ridges and graben in the basin interior plains (Watters et al., 2009-this issue). A notable regional-scale difference in the distribution of tectonic features is the density of wrinkle ridges in plains material exterior to the Caloris basin. A large number of wrinkle ridges are found in the exterior annulus of smooth plains to the east of the Caloris basin, but there are far fewer wrinkle ridges in the corresponding plains to the west (Fig. 8A). This asymmetry may in part be a result of less than optimum lighting for the NAC images of the region (Fig. 8B). The apparent difference in the number of wrinkle ridges to the east and west of Caloris is discussed in greater detail elsewhere (Watters et al., 2009-this issue).

6. Estimates of horizontal shortening

Previous estimates of horizontal shortening across lobate scarps on Mercury were limited to inferences derived from the maximum topographic relief and assumptions regarding the geometry of scarp-associated thrust faults (Watters et al., 1998, 2002). Crosscut impact craters provide the potential for more direct measures of horizontal shortening. In the area viewed by Mariner 10, craters crosscut by lobate scarps are generally greater than 30 km in diameter, and the amount of shortening across lobate scarps is not sufficiently large to be easily quantified on the basis of deformation of such craters (Watters et al., 1998).

MESSENGER NAC images have revealed three craters with diameters less than 30 km crosscut by lobate scarps. In addition to deforming the large elliptically shaped Sveinsdóttir crater, the north–south-trending segment of Beagle Rupes crosscuts a ~17-km-diameter crater (Fig. 2B). Although the shadow cast from Beagle Rupes obscures a portion of the rim and floor, the crater appears to have been overthrust, and a portion of the eastern rim of the crater may be vertically offset (Fig. 2B). The difference between the original crater diameter, inferred from the distance from rim to rim measured parallel to the strike of the scarp, and the shortened diameter, the distance from rim to rim measured perpendicular to the local strike of the scarp, is ~1 km. A kilometer of horizontal shortening at this location of the Beagle Rupes thrust fault is

Fig. 8. Tectonic feature map of Mercury, including areas imaged by MESSENGER and Mariner 10. (A) This map shows the distribution of lobate scarps (black), high-relief ridges (green), wrinkle ridges (blue), and graben (red). (B) The mapped tectonic features are overlaid on MESSENGER NAC and Mariner 10 mosaics. Where there is overlap in the images, the NAC mosaics are superimposed on the Mariner 10 hemispheric mosaic. The tectonic map combines previously digitized structures identified in Mariner 10 images (Watters et al., 2004; Watters and Nimmo, in press) with those newly identified from MESSENGER images.

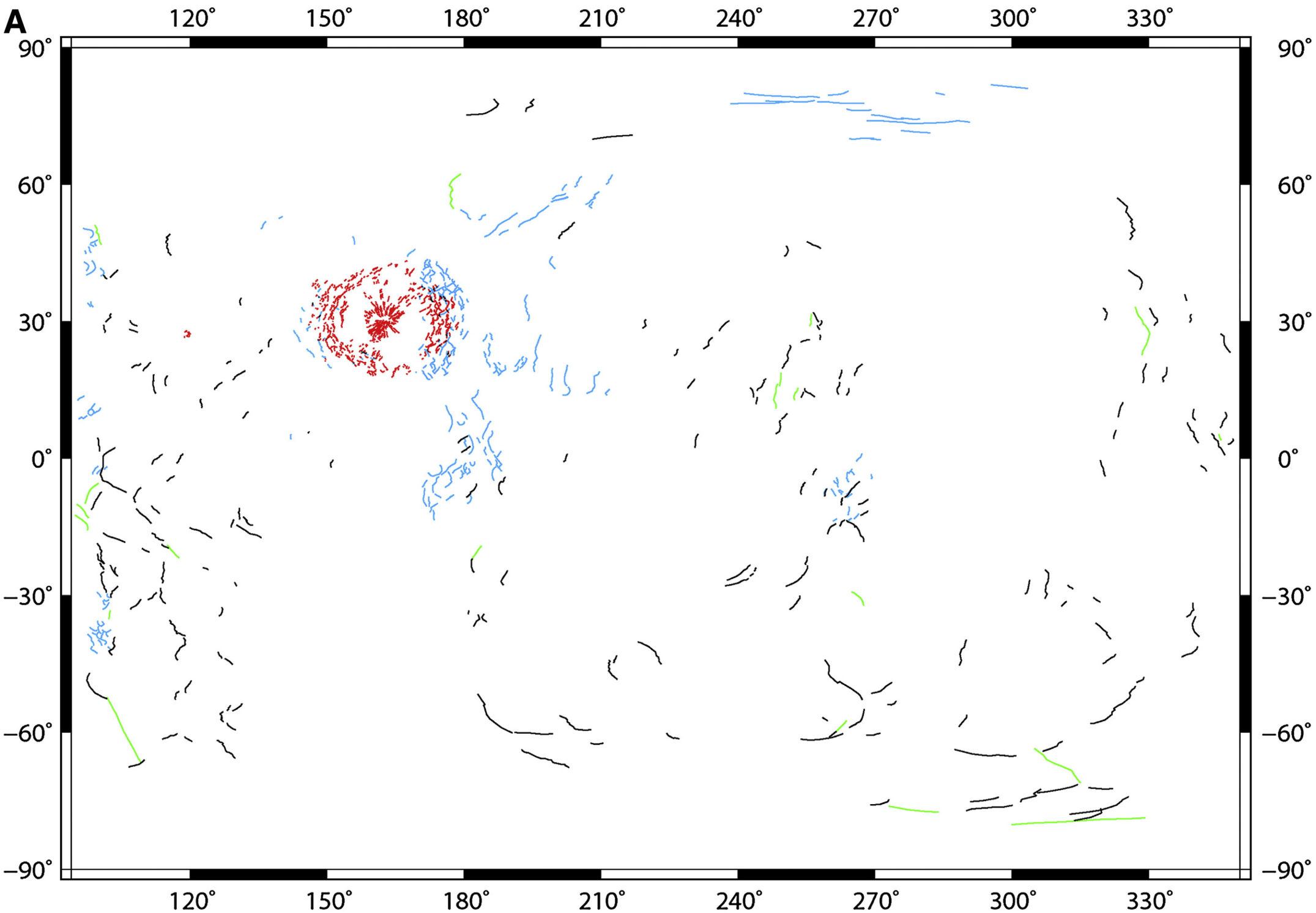
A
120°
150°
180°
210°
240°
270°
300°
330°
90°
60°
30°
0°
−30°
−60°
−90°

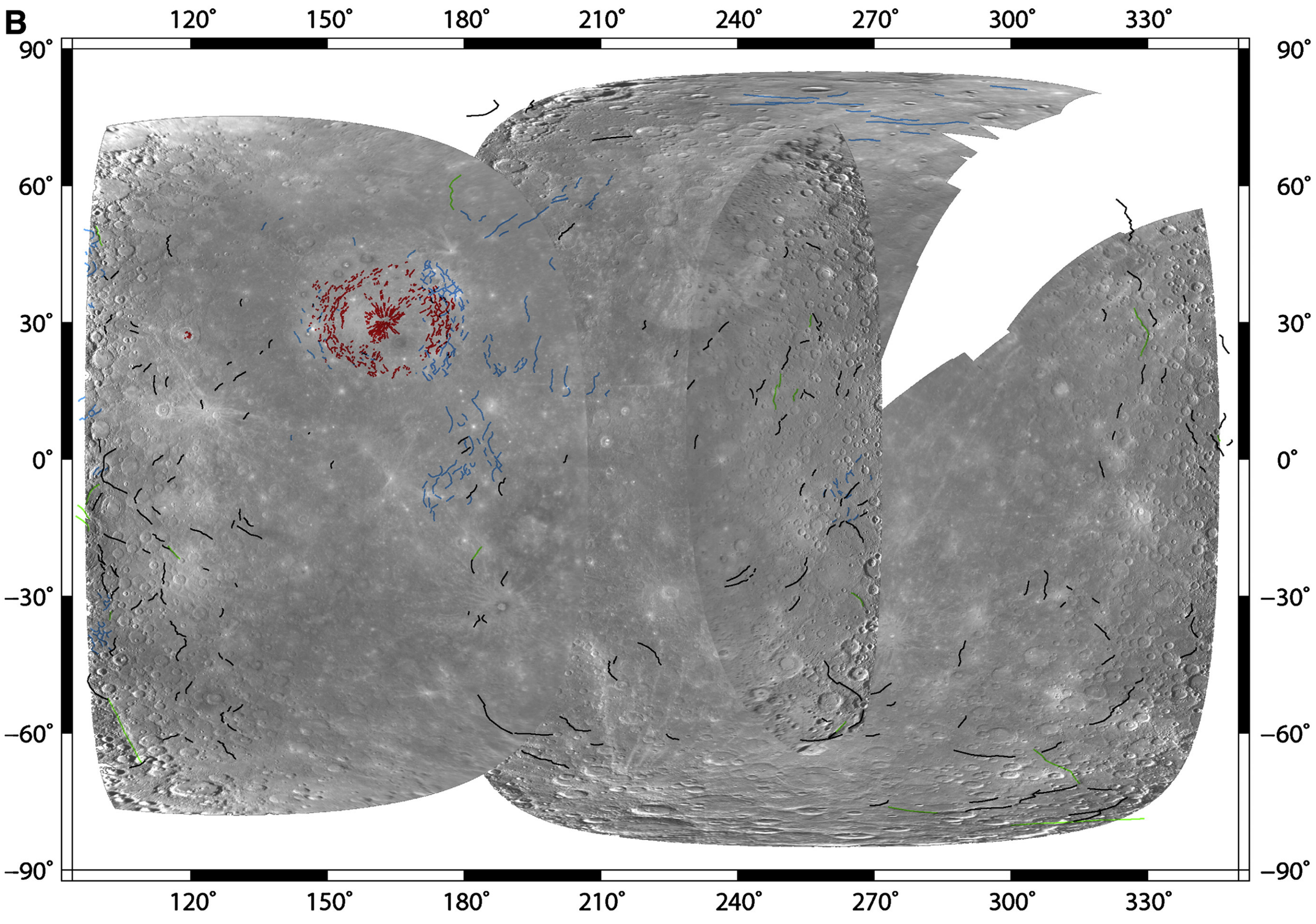
B
120°
150°
180°
210°
240°
270°
300°
330°
90°
60°
30°
0°
−30°
−60°
−90°

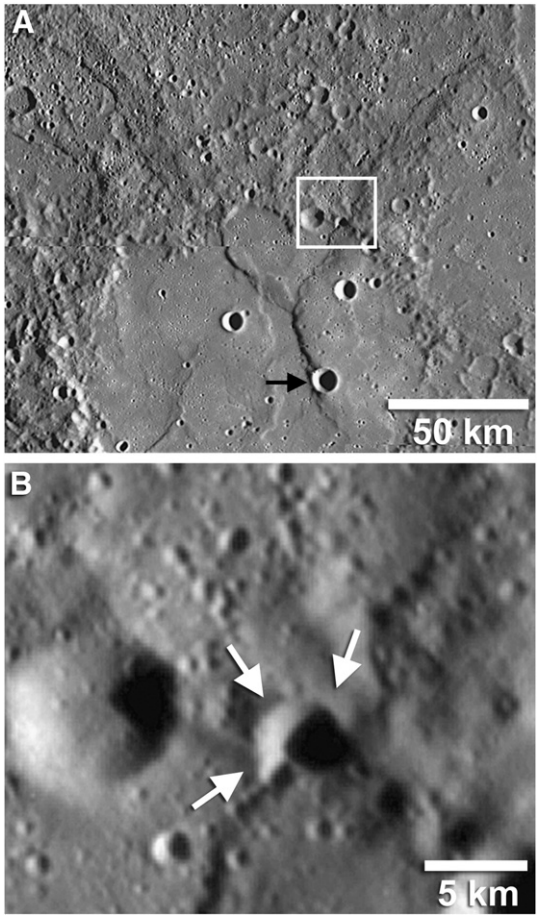

Fig. 9. Small impact crater overthrust by a lobate scarp. (A) A ~5-km-diameter impact crater located near the rim of a larger degraded impact crater is crosscut by the northeast–southwest-trending segment of a lobate scarp. A ~9-km-diameter impact crater is superposed on the southern segment of the scarp (black arrow). The resolution of the mosaic is 210 m/pixel. (B) Parts of the rim and floor of this relatively fresh small-diameter crater (white arrows) have been overthrust by the fault scarp. Measurements from the crater rim to scarp face indicate ~2 km of horizontal shortening. The location of (B) is shown in (A).

likely a lower limit, because of an uncertainty in the dimension of the shortened crater arising from such factors as non-optimum illumination direction and long shadows.

The 160-km-length lobate scarp southeast of Beagle Rupes (Fig. 3) crosscuts a 5-km-diameter impact crater (Fig. 9A, B). The southeastern portions of the crater rim and walls have been overthrust. The shadow cast by the crater rim and the lobate scarp obscures the crater floor and portions of the scarp face (Fig. 9B). The difference between the original crater diameter, estimated parallel to the scarp face, and the estimated distance from the northwestern crater rim to the scarp face (largely obscured by shadow) suggests that horizontal shortening was ~2 km.

To the southeast is a northwest–southeast-trending lobate scarp ~250 km in length that crosscuts two impact craters (Fig. 10). The northwesternmost segment of the scarp appears to crosscut a ~38-km-diameter crater (Fig. 10A); the trace of the scarp is more evident through the southeastern rim of the crater than across its floor. The second crater is ~11 km in diameter, degraded, and crosscut by the middle segment of the lobate scarp (Fig. 10B). The northeastern rim and a portion of the crater floor are buried by overthrust intercrater plains material (Fig. 10B). The difference between the original crater diameter, estimated from the curvature of the remaining rim, and the shortened diameter, measured from the southwestern rim to the base of the scarp face, suggests that horizontal shortening was ~3 km.

Estimates of the amount of horizontal shortening obtained from measurements of the maximum relief of all but the longest of the lobate scarps viewed by Mariner 10 range from ~0.3 to 1.8 km, under the assumption that the scarp-associated thrust faults are planar and dip at an angle θ of 25° (Watters et al., 1998). The horizontal shortening across Discovery Rupes, one of the largest lobate scarps viewed by Mariner 10, given a measured maximum relief of 1.5 km and an assumed dip angle of 25°, is ~3.2 km (Watters et al., 1998). The range of horizontal shortening measured from the three overthrust craters imaged by MESSENGER (~1 to 3 km) is in good agreement with estimates obtained from the relief of lobate scarps viewed by Mariner 10.

7. Contractional strain and radius change

The number and distribution of lobate scarps provide clear evidence that the crust and lithosphere of Mercury have undergone widespread contraction, presumably global in scale. The crustal shortening and contractional strain expressed by the lobate scarps, extrapolated to the entire surface, have been used to estimate the radius change due to global contraction (Strom et al., 1975; Watters et al., 1998; Watters and Nimmo, in press). Two approaches have been taken to estimate the amount of contraction from the thrust faults, one from the average shortening along the length of each fault (Strom et al., 1975), and one from displacement-length scaling relations (Watters et al., 1998; Watters and Nimmo, in press). For an average throw of 1 km along the total length of all scarp-

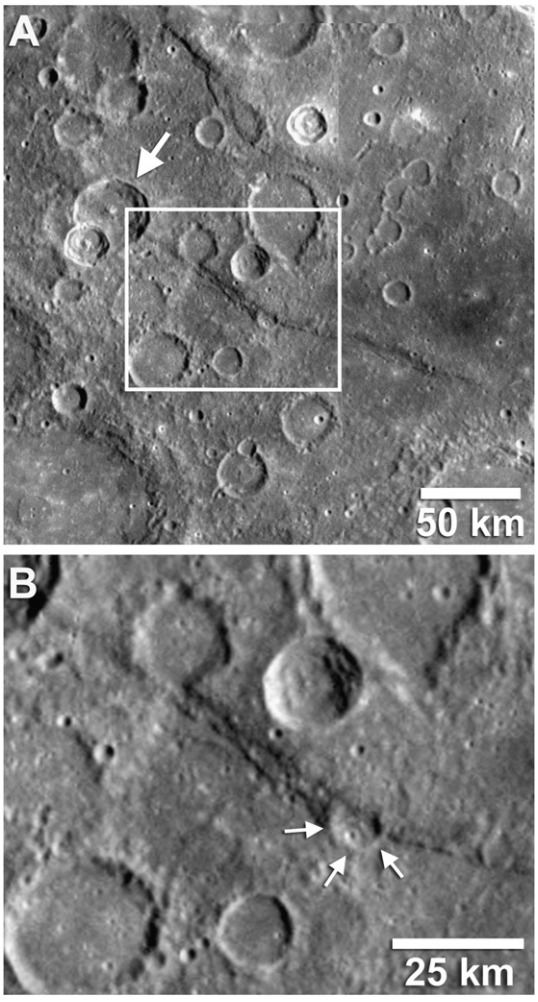

Fig. 10. Crosscut and overthrust impact crater. (A) A northwest-southeast-trending lobate scarp crosscuts a ~38-km-diameter crater (white arrow) and an ~11-km-diameter impact crater. The resolution of the mosaic is ~530 m/pixel. (B) Significant portions of the rim and floor of the 11-km-diameter crater (white arrows) have been overthrust. Measurements from the crater rim to scarp face indicate over 3 km of horizontal shortening near the middle of the lobate scarp. The location of (B) is shown in (A).

associated thrust faults and a fault plane dip angle θ of 25° to 45°, Strom et al. (1975) estimated that Mercury's radius decreased by 1 to 2 km. From the ratio γ of the estimated displacement to the measured fault length, Watters et al. (1998) determined the total contractional strain. The value of γ, determined from a linear fit to displacement-length data for large-scale lobate scarps characterized from Mariner 10 images, is $(6–8)\times10^{-3}$ for values of θ from 25° to 35°, with $\gamma \cong 6.9\times10^{-3}$ for $\theta = 30°$ (Watters and Nimmo, in press). For a given assumed value of average dip angle, the standard deviation in γ is approximately 50% (Watters et al., 2000), so ratios of slip to length on individual structures can easily deviate from the best-fit value by factors of 2 or more. Notwithstanding the spread in individual ratios, for the above range in γ and the total length of the mapped lobate scarps in Mariner 10 images (12,320 km), the areal contractional strain has been estimated to be 0.035–0.053% (0.043% for $\theta = 30°$) for the 45% of the surface imaged by Mariner 10 (Watters and Nimmo, in press). This range in the contractional strain corresponds to a radius decrease of approximately 0.4–0.6 km (~0.5 km for $\theta = 30°$) (Watters and Nimmo, in press). A maximum radius change of <1 km is consistent with previous estimates from a smaller area imaged by Mariner 10 (Watters et al., 1998) but is below the maximum estimate of Strom et al. (1975).

The discovery of previously unrecognized lobate scarps on the portion of Mercury's surface imaged by Mariner 10 indicates that the number and total length of thrust faults was underestimated. The cumulative length of 35 newly identified lobate scarps is 4090 km, bringing the total length of all the mapped scarps in the area seen by Mariner 10 to ~16,400 km. From the displacement-length scaling relation and the range of γ determined by Watters and Nimmo (in press), the average total contractional strain in the area viewed by Mariner 10 increases to 0.05–0.07% (0.06% for $\theta = 30°$). The total fault length, and thus the average contractional strain, is one third greater than previous estimates obtained using the same method (Solomon et al., 2008). The new average strain corresponds to a decrease in radius of about 0.6–0.8 km (~0.7 km for $\theta = 30°$). Because not all lobate scarps even in the area viewed by Mariner 10 hemisphere have been detected as a consequence of limitations imposed by lighting geometry, these new estimates of areal strain and radius change are only lower bounds.

The total length of the 72 lobate scarps identified in the area viewed for the first time by MESSENGER is ~8740 km. For the same range of γ, the average areal contractional strain for the 21% of the surface imaged for the first time by MESSENGER is ~0.05–0.07% (~0.06% for $\theta = 30°$). This range in strain, extrapolated to the entire surface, corresponds to a decrease in radius of about 0.6–0.9 km (~0.7 km for $\theta = 30°$). As with the area imaged by Mariner 10, these estimates are lower bounds because the lighting geometry was not optimum for all of the area imaged. The average contractional strain and implied radius change estimated from the total length of lobate scarps mapped in newly imaged regions by MESSENGER are thus comparable to those estimated from the population of known scarps in the portion of Mercury's surface seen by Mariner 10. Although the maximum radius change determined with the displacement-length scaling relation is still less than the maximum of 2 km estimated by Strom et al. (1975), it is likely that when global image coverage at near optimum lighting geometry is available from the orbital phase of the MESSENGER mission, and when additional new constraints on shortening from the deformation of small craters are obtained, the decrease in Mercury's radius subsequent to the end of heavy bombardment inferred from the population of lobate scarps will be in the range 1 to 2 km originally estimated by Strom et al. (1975).

8. Timing of deformation

The lobate scarps found in the area imaged for the first time by MESSENGER provide valuable new information on the timing of deformation. Lobate scarps seen in Mariner 10 images deform all major plains units on Mercury, and there is no clear evidence of embayment of lobate scarps by either the older intercrater plains or younger smooth plains. As described above, a first candidate embayment of a lobate scarp by smooth plains has been found in MESSENGER images (Fig. 3). The structural relief of a preexisting lobate scarp formed in older intercrater plains appears to have acted as a topographic barrier against which smooth plains material ponded. The low-relief ridges in the smooth plains flanking the scarp face may be evidence of continued movement on the thrust fault that underlies the scarp after the emplacement of the smooth plains (Fig. 3) (Solomon et al., 2008). This embayment relationship suggests that some lobate scarps formed after the emplacement of intercrater plains but prior to the emplacement of the smooth plains.

Impact craters crosscut by lobate scarps, particularly where scarps cut across small, fresh craters (Fig. 9), suggest that many of the thrust faults are Calorian in age or younger. However, the superposition of small impact craters on some lobate scarps, including those that crosscut other small impact craters (Figs. 2B, 3), makes a clear determination of the age relationship difficult. Some of the most compelling evidence for a relatively young age for the lobate scarps is their crosscutting relationship with smooth plains material. As is the case for Beagle Rupes (Fig. 2A) and the 160 km-long lobate scarp to the southeast (Fig. 3), lobate scarps clearly crosscut the smooth plains that fill impact basins and appear to postdate the wrinkle ridges that also deform these plains. These observations suggest that the thrust faulting that formed the lobate scarps began before the end of smooth plains emplacement and continued after the emplacement of the youngest smooth plains material (Solomon et al., 2008). At least some lobate scarps may be among the youngest landforms on Mercury.

9. Implications for thermal history

The contractional strain expressed by the lobate scarps, the associated planetary contraction, and the timing of surface faulting together provide important constraints on thermal history models for Mercury (Solomon, 1976, 1977, 1978, 1979; Schubert et al., 1988; Phillips and Solomon, 1997; Hauck et al., 2004). Most thermal history models for Mercury predict more radial contraction than can be accommodated by the mapped lobate scarps. Complete solidification of Mercury's core from an initially molten state, for instance, would lead to a reduction in planetary radius of about 17 km (Solomon, 1976). This magnitude of corresponding surface contractional strain is much larger than has been inferred from the known populations of lobate scarps. The onset time of inner core solidification, however, is not known and could readily have preceded the end of heavy bombardment. Any record of an early stage of crustal deformation from core solidification prior to about 3.8–4 Ga would therefore not be preserved. Thermal history models by Hauck et al. (2004) show that 1–2 km of radial contraction since 4 Ga can be met only for a limited subset of models, particularly those for which convective flow in the mantle is governed by a rheology appropriate to anhydrous olivine and the core contains a substantial weight fraction of sulfur (>6.5%) or another light element to retard the growth of the inner core.

Even for the global contraction that occurred after the end of heavy bombardment and the emplacement of the intercrater plains, horizontal shortening across lobate scarps may express only a fraction of the total strain. Dombard et al. (2001), for instance, suggested that long-wavelength (>100 km), low-amplitude lithospheric folds, not visible in Mariner 10 images, may have accommodated horizontal contraction comparable to that recorded by the lobate scarps. Pritchard and Stevenson (2000) discussed the parallel issue of whether the global contraction predicted by thermal evolution models for the Moon might have been accommodated despite the absence of a global distribution of major contractional features on the lunar surface.

The increase in total accumulated contraction since the end of heavy bombardment, compared with estimates derived only from

Mariner 10 observations, widens the suite of thermal history models consistent with Mercury's deformational history, as will further increases to total contraction that are set as additional imaging of the surface at low solar illumination reveals lobate scarps and other tectonic features not previously recognized. Moreover, the new constraints on the relative timing of scarp activity, plains formation, and impact cratering promise further constraints on the history of planetary contraction, most notably including the history of inner core growth and its implications as a source to power a magnetic dynamo in Mercury's outer core (Solomon et al., 2008).

10. Conclusions

The tectonic landforms revealed by the first MESSENGER flyby of Mercury have validated the prediction, made on the basis of Mariner 10 images (Strom et al., 1975), that contractional deformation has dominated the tectonic history of the innermost planet. Of the three classes of tectonic features that express crustal shortening on Mercury (lobate scarps, high-relief ridges, and wrinkle ridges), lobate scarps are the most widespread and have accommodated the greatest strain. Among the lobate scarps newly imaged by MESSENGER is one of the largest yet discovered on Mercury (Solomon et al., 2008). MESSENGER also documented the largest high-relief ridge on Mercury seen to date. Wrinkle ridges are common tectonic features in smooth plains material. The largest expanses of ridged plains (i.e., smooth plains with wrinkle ridges) occur within the interior of the Caloris basin and in its eastern exterior annulus. MESSENGER images show that wrinkle ridges are also found in smooth plains that fill the interior of smaller impact basins and larger craters. Wrinkle-ridge rings, circular patterns of wrinkle ridges in smooth plains occupying topographic lows, likely reflect the influence of shallowly buried impact craters, supporting a volcanic origin for smooth plains material (Head et al., 2008).

Extensional deformation has been found to date in only two locations on Mercury. Extensional faulting within the Caloris basin had been well documented by Mariner 10, but only for less than half of the basin interior. MESSENGER demonstrated that extensional fault structures occur throughout the Caloris interior and discovered that the center of the basin is marked by a radial pattern of graben, Pantheon Fossae, not seen elsewhere on the planet. MESSENGER also obtained the first clear evidence of extensional faulting outside of the Caloris basin smooth plains inside the peak ring of the comparatively youthful Raditladi basin.

A map of the distribution of tectonic features displays broad longitudinal bands containing many lobate scarps separated by adjacent bands with relatively few scarps. The latter bands generally correspond to areas with lighting geometry not optimal for recognizing low-relief features. The known distribution of tectonic features on Mercury may therefore be strongly biased by lighting geometry.

MESSENGER has revealed a number of small impact craters that have been crosscut and overthrust by lobate scarps. The horizontal shortening estimated from these craters ranges from ~1 to 3 km. The detection of previously unrecognized lobate scarps in areas imaged by Mariner 10 indicates that earlier estimates of contractional strain based on fault displacement-length scaling relations are too low. The average areal contractional strain is ~0.06%, about one third greater than the value determined previously by the same methodology. This accumulated strain corresponds to a decrease in Mercury's radius of as much as 0.8 km. These new estimates of strain and radius change are lower bounds because of the likelihood that not all lobate scarps have been recognized even in the areas imaged to date. New observations of crosscutting and embayment relations suggest that the thrust faults that produced the lobate scarps formed before the end of smooth plains emplacement and continued to be active after the emplacement of the youngest smooth plains material (Solomon et al., 2008). This inference suggests that some lobate scarps are relatively young, perhaps among the youngest endogenic landforms on Mercury. These comparatively young lobate scarps may constitute an expression of the slow but continuous radial contraction that accompanied the cooling of Mercury's interior and the growth of the planet's solid inner core.

Acknowledgements

We thank Matthew Golombek and Francis Nimmo for helpful comments that improved the manuscript. The MESSENGER project is supported by the NASA Discovery Program under contracts NASW-00002 to the Carnegie Institution of Washington and NAS5-97271 to the Johns Hopkins University Applied Physics Laboratory.

References

Cordell, B.M., Strom, R.G., 1977. Global tectonics of Mercury and the Moon. Phys. Earth Planet. Inter. 15, 146–155.
Dombard, A.J., Hauck, S.A., 2008. Despinning plus global contraction and the orientation of lobate scarps on Mercury: predictions for MESSENGER. Icarus 198, 274–276.
Dombard, A.J., Hauck, S.A., Solomon, S.C., Phillips, R.J., 2001. Potential for long-wavelength folding on Mercury. Lunar Planet. Sci. 32, abstract 2035.
Dzurisin, D., 1978. The tectonic and volcanic history of Mercury as inferred from studies of scarps, ridges, troughs, and other lineaments. J. Geophys. Res. 83, 4883–4906.
Freed, A.M., Solomon, S.C., Watters, T.R., Phillips, R.J., Zuber, M.T., 2009. Could the Pantheon Fossae be the result of the Apollodorus crater-forming impact within the Caloris basin, Mercury? Earth Planet. Sci. Lett. 285, 320–327 (this issue).
Golombek, M.P., Plescia, J.B., Franklin, B.J., 1991. Faulting and folding in the formation of planetary wrinkle ridges. Proc. Lunar Planet. Sci. Conf. 21, 679–693.
Hauck, S.A., Dombard, A.J., Phillips, R.J., Solomon, S.C., 2004. Internal and tectonic evolution of Mercury. Earth Planet. Sci. Lett. 222, 713–728.
Hawkins, S.E., Boldt, J., Darlington, E.H., Espiritu, R., Gold, R., Gotwols, B., Grey, M., Hash, C., Hayes, J., Jaskulek, S., Kardian, C., Keller, M., Malaret, E., Murchie, S.L., Murphy, P., Peacock, K., Prockter, L., Reiter, A., Robinson, M.S., Schaefer, E., Shelton, R., Sterner, R., Taylor, H., Watters, T., Williams, B., 2007. The Mercury Dual Imaging System (MDIS) on the MESSENGER spacecraft. Space Sci. Rev. 131, 247–338.
Head, J.W., Murchie, S.L., Prockter, L.M., Robinson, M.S., Solomon, S.C., Strom, R.G., Chapman, C.R., Watters, T.R., McClintock, W.E., Blewett, D.T., Gillis-Davis, J.J., 2008. Volcanism on Mercury: evidence from the first MESSENGER flyby. Science 132, 69–72.
Head, J.W., Murchie, S.L., Prockter, L.M., Solomon, S.C., Strom, R.G., Chapman, C.R., Watters, T.R., Blewett, D.T., Gillis-Davis, J.J., Fassett, C.I., Dickson, J.L., Hurwitz, D.M., Ostrach, L.R., 2009. Evidence for intrusive activity on Mercury from the first MESSENGER flyby. Earth Planet. Sci. Lett. 285, 251–262 (this issue).
King, S.D., 2008. Pattern of lobate scarps on Mercury's surface reproduced by a model of mantle convection. Nat. Geosci. 1, 229–232.
Matsuyama, I., Nimmo, F., 2009. Gravity and tectonic patterns of Mercury: the effect of tidal deformation, spin-orbit resonance, non-zero eccentricity, despinning and reorientation. J. Geophys. Res. 114, E01010.
Melosh, H.J., 1977. Global tectonics of a despun planet. Icarus 31, 221–243, this issue.
Melosh, H.J., Dzurisin, D., 1978. Mercurian global tectonics: a consequence of tidal despinning? Icarus 35, 227–236.
Melosh, H.J., McKinnon, W.B., 1988. The tectonics of Mercury. In: Vilas, F., Chapman, C.R., Matthews, M.S. (Eds.), Mercury. University of Arizona Press, Tucson, Ariz., pp. 374–400.
Murchie, S.L., Watters, T.R., Robinson, M.S., Head, J.W., Strom, R.G., Chapman, C.R., Solomon, S.C., McClintock, W.E., Prockter, L.M., Domingue, D.L., Blewett, D.T., 2008. Geology of the Caloris basin, Mercury: a new view from MESSENGER. Science 321, 73–76.
Pechmann, J.B., Melosh, H.J., 1979. Global fracture patterns of a despun planet: application to Mercury. Icarus 38, 243–250.
Phillips, R.J., Solomon, S.C., 1997. Compressional strain history of Mercury. Lunar Planet. Sci. 28, 1107–1108.
Pritchard, M.E., Stevenson, D.J., 2000. Thermal aspects of a lunar origin by giant impact. In: Canup, R., Righter, K. (Eds.), Origin of the Earth and Moon. University of Arizona Press, Tucson, Ariz., pp. 179–196.
Schubert, G., Ross, M.N., Stevenson, D.J., Spohn, T., 1988. Mercury's thermal history and the generation of its magnetic field. In: Vilas, F., Chapman, C.R., Matthews, M.S. (Eds.), Mercury. University of Arizona Press, Tucson, Ariz., pp. 429–460.
Schultz, R.A., 2000. Localization of bedding-plane slip and backthrust faults above blind thrust faults: keys to wrinkle ridge structure. J. Geophys. Res. 105, 12035–12052.
Solomon, S.C., 1976. Some aspects of core formation in Mercury. Icarus 28, 509–521.
Solomon, S.C., 1977. The relationship between crustal tectonics and internal evolution in the Moon and Mercury. Phys. Earth Planet. Inter. 15, 135–145.
Solomon, S.C., 1978. On volcanism and thermal tectonics on one-plate planets. Geophys. Res. Lett. 5, 461–464.
Solomon, S.C., 1979. Formation, history and energetics of cores in the terrestrial planets. Phys. Earth Planet. Inter. 19, 168–182.
Solomon, S.C., McNutt, R.L., Watters, T.R., Lawrence, D.J., Feldman, W.C., Head, J.W., Krimigis, S.M., Murchie, S.L., Phillips, R.J., Slavin, J.A., Zuber, M.T., 2008. Return to Mercury: a global perspective on MESSENGER's first Mercury flyby. Science 321, 59–62.
Spudis, P.D., Guest, J.E., 1988. Stratigraphy and geologic history of Mercury. In: Vilas, F., Chapman, C.R., Matthews, M.S. (Eds.), Mercury. University of Arizona Press, Tucson, Ariz., pp. 118–164.
Strom, R.G., Trask, N.J., Guest, J.E., 1975. Tectonism and volcanism on Mercury. J. Geophys. Res. 80, 2478–2507.

Strom, R.G., Chapman, C.R., Merline, W.J., Solomon, S.C., Head, J.W., 2008. Mercury cratering record viewed from MESSENGER's first flyby. Science 321, 79–81.
Thomas, P.G., Masson, P., Fleitout, L., 1988. Tectonic history of Mercury. In: Vilas, F., Chapman, C.R., Matthews, M.S. (Eds.), Mercury. University of Arizona Press, Tucson, Ariz., pp. 401–428.
Watters, T.R., 1988. Wrinkle ridge assemblages on the terrestrial planets. J. Geophys. Res. 93, 10236–10254.
Watters, T.R., 1993. Compressional tectonism on Mars. J. Geophys. Res. 98, 17049–17060.
Watters, T.R., Nimmo, F., in press. The tectonics of Mercury. In Watters, T.R., Schultz, R.A. (Eds.), Planetary Tectonics. Cambridge University Press, Cambridge, UK.
Watters, T.R., Robinson, M.S., Cook, A.C., 1998. Topography of lobate scarps on Mercury: new constraints on the planet's contraction. Geology 26, 991–994.
Watters, T.R., Schultz, R.A., Robinson, M.S., 2000. Displacement-length relations of thrust faults associated with lobate scarps on Mercury and Mars: comparison with terrestrial faults. Geophys. Res. Lett. 27, 3659–3662.
Watters, T.R., Robinson, M.S., Cook, A.C., 2001. Large-scale lobate scarps in the southern hemisphere of Mercury. Planet. Space Sci. 49, 1523–1530.
Watters, T.R., Schultz, R.A., Robinson, M.S., Cook, A.C., 2002. The mechanical and thermal structure of Mercury's early lithosphere. Geophys. Res. Lett. 29, 1542. doi:10.1029/2001GL014308.
Watters, T.R., Robinson, M.S., Bina, C.R., Spudis, P.D., 2004. Thrust faults and the global contraction of Mercury. Geophys. Res. Lett. 31, L04071. doi:10.1029/2003GL019171.
Watters, T.R., Nimmo, F., Robinson, M.S., 2005. Extensional troughs in the Caloris basin of Mercury: evidence of lateral crustal flow. Geology 33, 669–672.
Watters, T.R., Murchie, S.L., Robinson, M.S., Solomon, S.C., Denevi, B.W., André, S.L., Head, J.W., 2009. Emplacement and tectonic deformation of smooth plains in the Caloris basin, Mercury. Earth Planet. Sci. Lett. 285, 309–319 (this issue).